Brodogradnja Volume 75, Number 2 (2024) 75207

journal homepage: www.brodogradnja.fsb.hr

Brodogradnja

An International Journal of Naval Architecture and Ocean Engineering for Research and Development

Research on optimal design of 6in offshore flange connector's sealing structure

Jianguo Qin[1], Minghui Ji[1], Haixia Gong[2], Sijia Guo[3], Yanfeng Zhang[1], Yejiang Li[4], Haitang Cen[1]*

[1] *School of Mechanical Engineering, Inner Mongolia University of Technology, 010051 Hohhot, China*
[2] *School of Mechanical and Electrical Engineering, Harbin Engineering University, 150001 Harbin, China*
[3] *School of Mechanical Engineering, Jiamusi University, 154007 Jiamusi, China*
[4] *Ningbo Runsheng Intelligent Technology Co., Ltd., 315800 Ningbo, China*

ARTICLE INFO

Editor-in-Chief: Prof. Nastia Degiuli
Associate Editor: PhD Ivana Martić

Keywords:
Structural parameters
Maximum contact pressure
Optimal design model
Sealing performance

ABSTRACT

Taking the maximum contact pressure as the objective function for, the optimal design model of the offshore flange connector was established to analyze the impact of the flange cone's angle and the curvature radius of the lenticular gasket's contact surface on the sealing performance of the connector. An optimized three-dimensional model of the offshore flange connector was constructed using the MATLAB software's fmincon function to obtain the optimal size of the cone angle and curvature radius. The maximum contact pressure and maximum equivalent stress values of the non-optimized and optimized offshore flange connectors under the cross combination of two design pressures and six operating temperatures were analyzed by Workbench software, and the sealing performance of the non-optimized and optimized offshore flange connectors was compared according to the sealing judgment basis. The results show that compared with the previously studied offshore flange connector, the sealing structure of optimized offshore flange exhibits maximum increase in contact pressure increase but maximum decrease in equivalent stress. Under actual operating circumstances, the optimized offshore flange connection performs better in sealing and is less prone to breakage.

1. Introduction

With the depletion of onshore oil resources, oil extraction is gradually shifted from land to sea. One of the most crucial mechanical components for the exploitation of undersea oil resources is offshore production system, which consists of submarine pipelines and their connectors [1,2]. One of the key components in the leakage of offshore oil production equipment is offshore flange connector, which mainly serves to divert offshore oil pipelines and repair pipeline ruptures, and it is mainly comprised of flange, lenticular gasket, and bolt [3,4]. The offshore flange connector is often used for submarine pipeline connection at a water depth of about 500 meters, where most of the connections of offshore flange connectors are directly controlled by divers, or offshore sealing chamber is used as a workspace to connect undersea working machinery. Under the influence of bolt preload, the two flanges pinch the lenticular gasket such that the curved surface of the gasket and the conical surface of the flange are in close contact, producing the main body of a sealing structure.

* Corresponding author.
E-mail address: 2245412001@qq.com

http://dx.doi.org/10.21278/brod75207
Submitted 25 August 2023; Accepted 26 February 2024;
ISSN 0007-215X; eISSN 1845-5859

Since offshore flange connector will withstand the effect of internal high temperature oil and gas medium and external seawater pressure load for a long time, its sealing structure will deform and fail, resulting in leakage. Therefore, the contact surface of the sealing structure must be under sufficient pressure to suffer plastic deformation [5]. Thus, most of the microscopic concave and convex surfaces are tightly adhered to meet the sealing requirements [6]. Zhao [7] et al. analyzed and simulated the contact pressure of the metal sealing ring of the submarine X-TREE wellhead connector by using the mechanical analysis method of high pressure vessel sealing, and pointed out that the structural parameters of the metal sealing ring are the main factors affecting the change in contact pressure. Jing [8] et al. constructed the mathematical link between structural factors and contact pressure, and used this mathematical model as the goal function to optimize the X-O composite seal. Li [9] et al. analyzed the effects of the preload force, contact width, and working pressure on the sealing ring's contact pressure through finite element method and emerged to a theoretical conclusion about the relationship between the contact pressure and structural characteristics of the sealing ring of submarine wellhead connector. Guo [10] et al. explored the influence of structural parameters of a V-shaped sealing ring on its maximum contact pressure, and then used it as a design parameter to optimize the structure of the V-shaped sealing ring with the help of Workbench software. Yang [11] et al. established a numerical analysis model of O-ring seal with skeleton, obtained the optimal combination parameters to ensure sealing performance, and conformed the rationality of the sealing structure through experiments. Huang [12] et al. improved the performance of the seal significantly by using the finite element method to optimize the dip angles, width, and rear support structure of the metal ring sealing surface. Cheng [13] et al. used the control variable approach to study the impact of various structural parameters on the self-tightening metal U-shaped sealing ring's sealing performance and came up with the ideal structural size for the sealing ring to retain optimum sealing performance. Ren [14] et al. performed multi-objective optimization on VL sealing rings using Isight software, determined the optimal geometric size for the rings and enhanced their sealing capabilities.

According to the research results mentioned above, previous research was mostly focused on seals such as submarine wellhead connectors, but with little research on the structural optimization of offshore flange connector. Especially in the process of verifying the sealing performance of the optimized submarine well connector, the impact of the operating temperature factors of the extracted crude oil on its sealing performance is not taken into account. However, one of the essential elements influencing metal sealing performance is sealing structure mentioned in the aforementioned literature, which provides a theoretical reference for the optimization of the sealing structure of the offshore flange connector constructed in this paper.

In light of the aforementioned issues, this research improved the sealing structure of offshore flange connector, established its corresponding three-dimensional model, and utilized MATLAB's fmincon function to obtain the optimal sealing structure size [15]. Furthermore, the maximum contact pressure and maximum equivalent stress values of non-optimized and optimized flange connectors were analyzed by Workbench software under two design pressures and six temperature conditions. The results indicated that the optimized offshore flange connector had better sealing performance in actual working conditions.

2. Sealing principle and sealing judgment basis of offshore flange connector

2.1 Sealing structure and sealing principle of offshore flange connector

Figure 1 depicts the structural layout of offshore flange connector. Its sealing function is achieved by tightening the bolt with offshore operation tool, causing the curved surface on both sides of the lenticular gasket and the contact cone of the two flanges to form a sealing structure under the action of bolt preloading force.

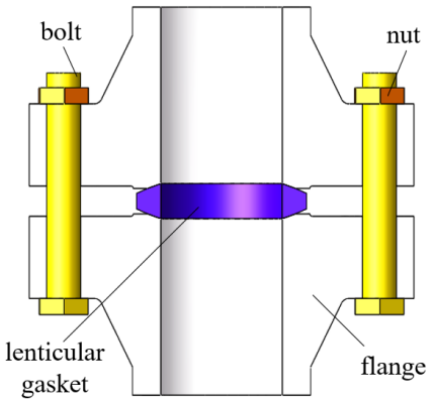

Fig.1 Diagram of the offshore flange connector's structure

2.2 Sealing judgment basis for offshore flange connector

The offshore flange connector has been working in an environment with high temperatures and pressures for a long time, and its sealing form is dominated by metal-to-metal contact sealing. The sealing pressure ratio defines the unit area of pressure applied to the sealing surface and is an essential indicator that reflects the metal sealing performance. The higher the sealing pressure ratio, the more pressure there has to be on the unit surface, the better the sealing performance. The sealing pressure ratio of the flange and the lenticular gasket are correlated with maximum contact pressure [16] in the contact process, which is expressed as:

$$P_{\max} = \frac{4P_{\mathrm{m}}}{\pi} \tag{1}$$

where $P_{\max}$ is the maximum pressure value of the contact surface between the flange and the lenticular gasket, MPa; P_{m} is the sealing pressure ratio, MPa.

The formula shows that the maximum pressure of the sealing surface is proportional to its sealing pressure ratio. Under the premise of not exceeding the tensile strength of the material, the greater the specific pressure of the sealing surface, the greater the maximum contact pressure, and the better the metal sealing performance. Thus, maximum contact pressure may be used as a direct indicator of sealing performance. Studies have shown that the contact pressure between the two metals must be higher than double the yield strength of the softer metal materials in order to create an efficient metal sealing [17]. Wang [18] et al. proved the rationality of the sealing determination basis through the theoretical derivation of the elastoplastic contact model. Moreover, Buchter [19] also proved the accuracy of the decision basis through experiments.

As the hardness of the flange is greater than that of the lenticular gasket, the yield strength of the lenticular gasket material is taken as a reference. At the same time, the contact pressure of the sealing surface must be lower than the material's tensile strength so as to prevent the lenticular gasket from fracturing. Although the yield strength of the lenticular gasket material will decrease as operating temperature rises, this will not affect the results of the study. Due to the selection of the yield strength of lenticular gasket under low-temperature working conditions, this value is too large, making seal judgment reference value also too high. If the sealing structure under high-temperature conditions can meet the judgment basis of low-temperature conditions, it will also satisfy the judgment basis under high temperatures. Therefore, the sealing judgment basis established in this paper is that the contact pressure of the sealing surface is between the tensile strength and twice the yield strength of the lenticular gasket material, and the greater the contact pressure of the sealing surface in this range, the better the sealing performance.

3. The geometric model and optimal design model of offshore flange connector

3.1 Geometric model of flange and lenticular gasket

Using the German DIN2627 flange design standard as a guide and referring to the structural sizes of 6in flanges, a geometric model for flange is designed in this study. There are 12 bolt holes on the flange. The construction and assembly schematic of the flange are shown in Figure 2.

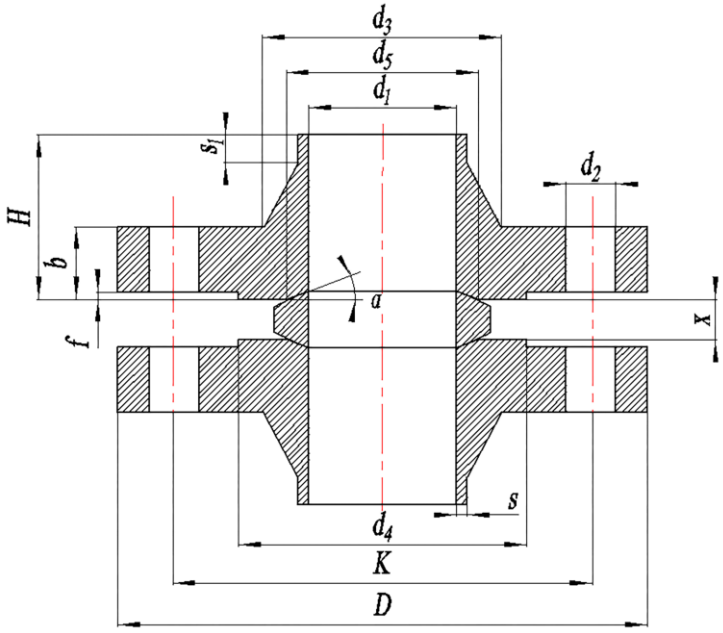

Fig.2 Structure design and assembly diagram of flange

As shown in Figure 2, d_1 is the inner diameter of the flange, d_2 is the diameter of the bolt hole; d_4 is the boss diameter of the flange; f is the height of the boss; b is the height of the bolt hole; H is the height of the whole flange; s is the thickness of the pipe wall; x is the distance between the upper and lower flange ends, which is 26 mm; d_5 is the diameter of the bottom of the flange contact cone; and the angle of the flange contact cone is 20°. The structural dimensions of the flange are shown in Table 1, unit is mm.

Table 1 Flange's dimensions

d_1	d_2	d_3	d_4	d_5	D	K	S	S_1	f	b	H
150	42	302	218	183	475	390	35	35	3	105	200

With reference from the German DIN2629 lenticular gasket design standard, Figure 3 displays the structural design of the lenticular gasket.

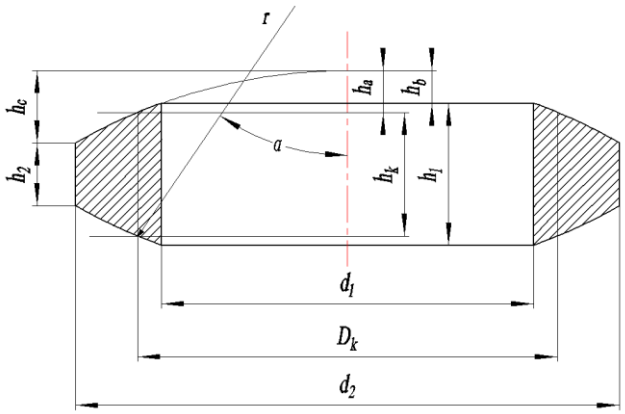

Fig.3 Structural design diagram of the lenticular gasket

As shown in Figure 3, d_1 is the inner diameter of the lenticular gasket, d_2 is the outer diameter of the lenticular gasket, D_k is the center circle diameter of the lenticular gasket, h_1 is the thickness of the inner wall of the lenticular gasket, h_2 is the thickness of the outer wall of the lenticular gasket, α is the angle of the flange contact cone, and r is the curvature radius of the lenticular gasket.

The contact center circle diameter D_k of the lenticular gasket and flange can be calculated by:

$$D_k = (d_1 + d_5)/2 \tag{2}$$

The contact surface of the lenticular gasket's curvature radius r, can be calculated by:

$$r = \frac{D_k}{2\cos(90° - \alpha)} \tag{3}$$

The thickness of the lenticular gasket contact center can be calculated by:

$$h_k = x + \frac{d_5 - D_k}{\tan 70°} \tag{4}$$

The inner wall thickness of the lenticular gasket can be calculated by:

$$h_1 = h_k + 2 \times h_b - 2 \times h_a \tag{5}$$

The exterior wall thickness of the lenticular gasket can be calculated by:

$$h_2 = h_k + 2 \times h_b - 2 \times h_c \tag{6}$$

where h_a, h_b, and h_c can be calculated using the following three formulas:

$$h_a = r - \frac{1}{2} \times \sqrt{4 \times r^2 - d_1^2} \tag{7}$$

$$h_b = r - \frac{1}{2} \times \sqrt{4 \times r^2 - D_k^2} \tag{8}$$

$$h_c = r - \frac{1}{2} \times \sqrt{4 \times r^2 - d_2^2} \tag{9}$$

The calculated structural dimensions of the lenticular gasket are shown in Table 2, and unit is mm.

Table 2 Dimensions of the lenticular gasket

D_k	r	d_1	d_2	h_1	h_2	h_k	h_a	h_b	h_c
166.2	243	150	210	37.7	13.7	32.1	11.86	14.65	23.86

3.2 Force analysis of sealing structure

Since both the flange and the lenticular gasket are axis-symmetric structures, their force states are likewise symmetrical. The force of lenticular gasket is analyzed in Figure 4.

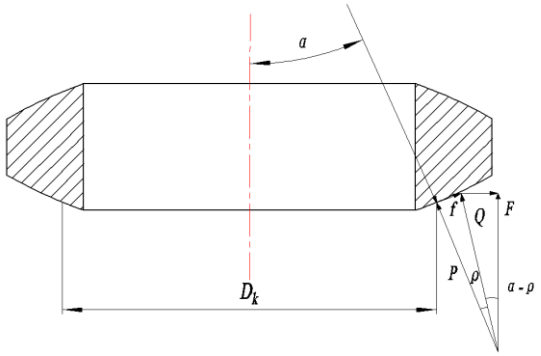

Fig.4 Diagram of the force acting on the lenticular gasket

The bolt preloading force F acts on the lenticular gasket, forming contact stress P on the sealing surface. The bolt preloading force in an operational condition [20] can be calculated by:

$$F = \frac{\sigma_s^2 \pi^2 r D_k \cos(\alpha - \rho)}{E^* \cos(\rho)} + \frac{\pi D_k^2}{4} q \tag{10}$$

where σ_s is the yield strength of lenticular gasket material, r is the contact surface's curvature radius, D_k is the diameter of the contact center circle, $\alpha = 20°$ is the flange's cone angle, $\rho = 8.5°$ is the angle of friction between the flange and the lenticular gasket, q is the designed pressure of the offshore flange connector, $q = 34.5$ MPa; E^* is the equivalent elastic modulus, and its relation is expressed as [21]:

$$\frac{1}{E^*} = \frac{1 - v_1^2}{E_1} + \frac{1 - v_2^2}{E_2} \tag{11}$$

E_1 and E_2 are the elastic modulus of the materials for the lenticular gasket and the flange, respectively; v_1 and v_2 are the poisson ratio of materials for the lenticular gasket and the flange, respectively, $v_1 = v_2 = 0.3$. According to Figure 4, F is bold preloading force, P is the normal component force of the lenticular gasket, and f is the tangential component force of the lenticular gasket. The force balance relationship can have the following outcomes:

$$P = \frac{F \cos(\rho)}{\cos(\alpha - \rho)} \tag{12}$$

The two-dimensional force of the contact between the lenticular gasket and the flange is analyzed in Figure 5.

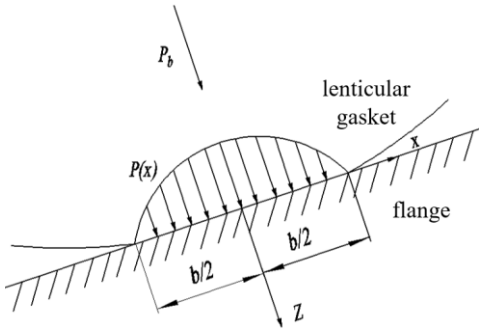

Fig.5 Two-dimensional contact force between the flange and the lenticular gasket

The initial contact between the flange and the lenticular gasket is line contact. The linear load P_b on the contact center circle between the flange and the lenticular gasket is expressed as:

$$P_b = \frac{P}{\pi D_k} = \frac{F \cos(\rho)}{\pi D_k \cos(\alpha - \rho)} \tag{13}$$

According to the two-dimensional contact theory of a cylinder in contact mechanics [22], the pressure distribution in the contact area between the flange and the lenticular gasket is give as:

$$p(x) = \frac{4P_b}{\pi b^2}(b^2 - x^2)^{1/2} \tag{14}$$

The maximum contact pressure occurs at the point of contact at $x = 0$, whose value can be calculated by:

$$p_0 = \frac{4P}{\pi b} = \left(\frac{P_b E^*}{\pi r}\right)^{1/2} = \frac{1}{\pi}\sqrt{\frac{FE^* \cos(\rho)}{r D_k \cos(\alpha - \rho)}} \tag{15}$$

As can be seen from formula (15), the contact pressure is influenced by the bolt pretightening force F as well as the sealing structural parameters r, and D_k. According to research, the contact pressure of the sealing surface is an important indicator affecting sealing performance. Therefore, sealing performance can be effectively improved by changing the structural configurations of the offshore flange connector [23].

The contact seal width b is calculated by:

$$b = \frac{4P_0 r}{E^*} = \frac{4}{\pi}\sqrt{\frac{Fcos(\rho)r}{E^* D_k cos(\alpha - \rho)}} \tag{16}$$

The sealing half width a is obtained. The normal distribution force $q(x)$ is applied within the width of the seal. Assuming any element to be ds, the stress caused by any point (x_0,z_0) in the lenticular gasket is expressed as:

$$\begin{cases} \sigma_{x_0} = -\dfrac{2Z_0}{\pi}\int_{-a}^{+a}\dfrac{p(x)(x_0 - s)^2 ds}{[(x_0 - s)^2 + Z_0^2]^2} \\ \sigma_{y_0} = \mu_1(\sigma_{x_0} + \sigma_{z_0}) \\ \sigma_{z_0} = -\dfrac{2Z_0^3}{\pi}\int_{-a}^{+a}\dfrac{p(x)ds}{[(x_0 - s)^2 + Z_0^2]^2} \end{cases} \tag{17}$$

By substituting formula (14) into formula (17) and integrating in the direction of the z_0 axis, the principal stress inside the contact region of the lenticular gasket can be obtained as:

$$\begin{cases} \sigma_{x_0} = -\dfrac{2P_b}{\pi a^2}[(a^2 + 2z_0^2)(a^2 + z_0^2)^{-\frac{1}{2}} - 2z_0] \\ \sigma_{y_0} = -\dfrac{4\mu_1 P_b}{\pi a^2}(\sqrt{a^2 + z_0^2} - z_0) \\ \sigma_{z_0} = -\dfrac{2P_b}{\pi}(a^2 + z_0^2)^{-\frac{1}{2}} \end{cases} \tag{18}$$

The maximum contact stress is calculated by:

$$\sigma_{max} = \frac{1}{\sqrt{2}}\sqrt{(\sigma_{x_0} - \sigma_{y_0})^2 + (\sigma_{y_0} - \sigma_{z_0})^2 + (\sigma_{z_0} - \sigma_{x_0})^2} \tag{19}$$

3.3 Optimal design model of sealing structure

By analyzing the maximum contact pressure, it is known that changing the sealing structure parameters can effectively improve the sealing performance of the offshore flange connector. Due to $D_k = 2r\cos(90° - \alpha) = 2r\sin(\alpha)$, formula (15) can be rewritten as:

$$p_0 = \frac{1}{\pi r}\sqrt{\frac{FE^* \cos(\rho)}{2\sin(\alpha)\cos(\alpha - \rho)}} = \frac{1}{\pi r}\sqrt{\frac{FE^* \cos(\rho)}{\sin(2\alpha - \rho) + \sin(\rho)}} \tag{20}$$

In this paper, ρ is the friction angle between metal and metal, which is invariable. It is feasible to enhance the contact pressure of the sealing surface while maintaining the same bolt preloading force by changing the angle of the flange contact cone and the curvature radius of the lenticular gasket, which will improve the sealing performance of the offshore flange connection. Therefore, the angle of the flange contact cone and the curvature radius of the lenticular gasket are used as design variables for the sealing structure optimization model, with formula (20) serving as the objective function.

Since the angle of the flange contact cone is between 0° and 90°, it can be obtained from the objective function that the smaller sin (2α-ρ) is, the larger P_0 is. P_0 increases in size as r, while the curvature radius of the lenticular gasket decreases. However, the size of the lenticular gasket imposes restrictions on both α and r. The values of α and r are subject to the following relationship because the contact center circle diameter D_k between the lenticular gasket and the cone of the flange lies between the inner diameter d_1 and the outer diameter d_2 of the lenticular gasket: $d_1 < D_k = 2r\sin(\alpha) < d_2$.

The sealing performance of the offshore flange connector is improved with the increase of objective function values. However, the value of P_0 should not be higher than the tensile strength of the lenticular gasket. Using the established sealing judgment basis for offshore flange connector, the following results may be attained: $2\sigma_s < P_0 < \sigma_b$.

The yield strength of lenticular gasket material is given in the formula above as σ_s, while its tensile strength is given as σ_b. The yield strength and tensile strength of the lenticular gasket, which is made of 316 stainless steel, are 205 MPa and 515 MPa, respectively. Hence, three sealing structure optimization parameters of the offshore flange connector can be obtained:

1. max $p_0 = \frac{1}{\pi r}\sqrt{\frac{FE^* \cos(\rho)}{\sin(2\alpha-\rho)+\sin(\rho)}}$
2. Subject to: 410Mpa < p_0 < 515 MPa
3. $D=[\alpha, r]$

D stands for design variable, 0°< α < 90°, 150 mm < 2$r$sin(α) < 210 mm. After the optimized design parameters are identified, the program is prepared in MATLAB. Figure 6 shows the comparative data of optimization parameters.

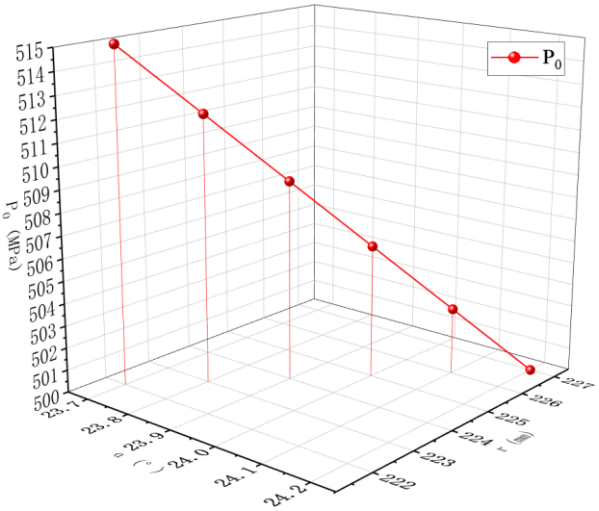

Fig.6 Comparative data for optimization parameters

As can be seen from Figure 6, the maximum P_0 value is 515 MPa, while the constraint conditions require P_0 to be less than 515 MPa, so the most reasonable P_0 value is 512 MPa, corresponding to the angle of the flange cone α of 23.8°, and the curvature radius of the lenticular gasket r of 223 mm. The structural dimensions of the optimized lenticular gasket are shown in Table 3, and unit is mm.

Table 3 Optimized dimensions of the lenticular gasket

D_k	r	d_1	d_2	h_1	h_2	h_k	h_a	h_b	h_c
180	223	150	210	37.8	11.2	26	13	18.9	26.3

It can be seen from formulas (18), (19) and (20) that changing the seal structure parameters α and r can change not only the contact pressure of the seal structure, but also the maximum equivalent stress. The maximum contact pressure reflects the stress of the contact surface, while the maximum equivalent stress reflects the stress of the whole sealing structure. The greater the maximum contact pressure of the contact surface does not necessarily mean the greater the maximum equivalent stress of the whole sealing structure. A series of z_0 values are substituted into formula (18), and finally formula (19) is calculated. σ_{max1} represents the equivalent stress before optimization, and σ_{max2} represents the equivalent stress after optimization, as shown in Table 4, unit is MPa. The maximum equivalent stress of the optimized sealing structure is calculated to be less than that of the non-optimized sealing structure, thus verifying the rationality of the finite element simulation results.

Table 4 Comparison of equivalent stress of sealing structure

z_0	1	1.5	2	2.5	3
σ_{max1}	63.9	48.36	38.115	31.23	26.378
σ_{max2}	62.52	46.39	36.33	29.68	25.03

4. Finite element analysis of non-optimized and optimized offshore flange connectors

4.1 Establishment of finite element analysis model of offshore flange connector

After the creation of non-optimized and optimized flange and lenticular gasket, build a three-dimensional model of the parts and assemble them with Soildworks was constructed. Due to the symmetry of the constructed offshore flange connection, a quarter of the offshore flange connector is utilized as the geometric model for finite element analysis, according to literature [24]. Symmetrical symmetry restrictions were placed on the two cutting sides of the geometric model, the mesh was further divided and refined on the contact surface between the lenticular gasket and the flange [25], as illustrated in Figure 7. In order to decrease the number of divided mesh and facilitate calculation, the model was imported into Workbench software for finite element analysis. The augmented Lagrange algorithm was adopted as the contact mode between the flange and the lenticular gasket to improve the calculation accuracy and convergence.

Table 5 Material properties of each part of the offshore flange connector

Part	Materials	Poisson ratio	elasticity modulus(Gpa)	Yield strength(MPa)
Flange	12Cr2Mo1	0.3	210	620
Lenticular gasket	316	0.3	201	205
Bolts and nuts	50Cr	0.3	210	930

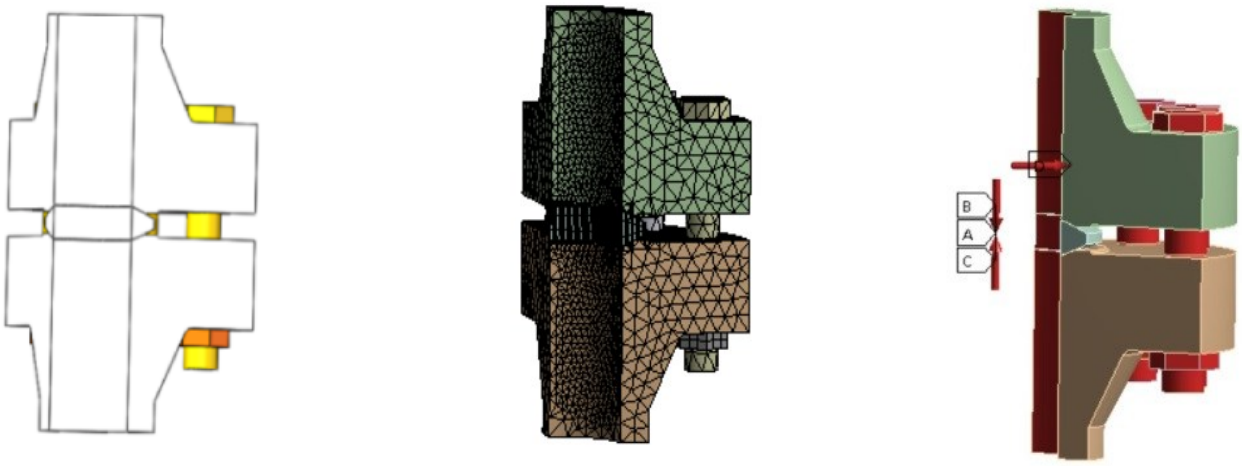

(a) Geometric model (b) Mesh generation (c) Boundary conditions

Fig.7 Modeling of finite element analysis

The bolt preloading force was computed using formula (10), and the average preload for each bolt was calculated to be 74.6 KN. The preloading force of 74.6 KN was respectively applied to the three bolts of the geometric model, and a medium pressures of 34.5 MPa and 41.4 MPa was respectively applied to the inner wall. Then the temperature of the sealing structure of the offshore flange connector was set according to six operating temperatures to finally calculate the contact pressure under these conditions. The material attribute of each component of the offshore flange connection is specified in Table 5.

4.2 Setting of boundary conditions and load constraints of offshore flange connector

As crude oil stored in the seabed is very viscous, it is necessary to transport high-temperature and high-pressure media in the oil production equipment to reduce the viscosity of the crude oil and further facilitate its exploitation. With the increase in medium transport temperature, oil production equipment generally has a temperature of higher than 100 °C, and even 150 °C [26]. At the same time, offshore flange connector is also affected by the pressure difference between the internal and external medium in the submarine operation process. Given the complexity of offshore oil production, the standard pressure difference for offshore connectors is generally 34.5 MPa. The safety factor is 1.2 times, that is, the design pressure under working conditions was set to 41.4 MPa [27]. The contact pressure of the sealing structure under the two pressure differences was then compared and analyzed. Therefore, the contact pressure of non-optimized and optimized sealing structures was explored under the two pressure conditions at the operating temperatures of 25 °C, 50 °C, 75 °C, 100 °C, 125 °C, and 150 °C.

4.3 Interpretation of result

The contact pressure of the sealing structures under the condition of six operating temperatures and two design pressures were solved using the statics module of Workbench software. The two extreme temperatures of each design pressure are provided as an example to precisely depict the contact pressure distribution between the flange and the lenticular gasket in the offshore flange connector. The cloud diagram of the contact pressure of non-optimized and optimized sealing structures at 25 °C and 125 °C under the design pressure of 34.5 MPa is given in Figure 8.

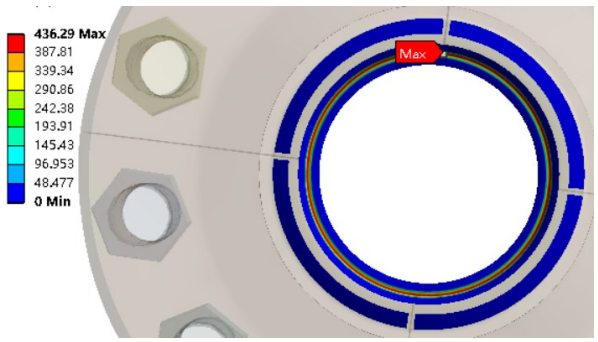

(a) Contact pressure cloud diagram of the non-optimized sealing structure at 25° C

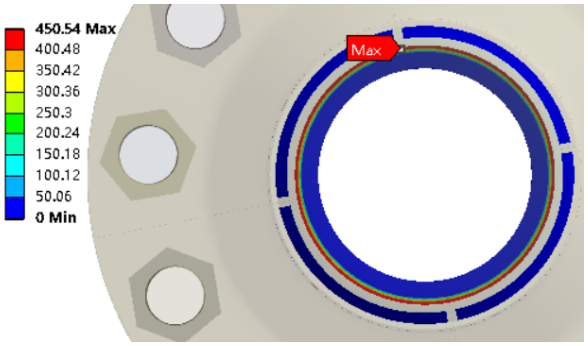

(b) Contact pressure cloud diagram of the optimized sealing structure at 25°C

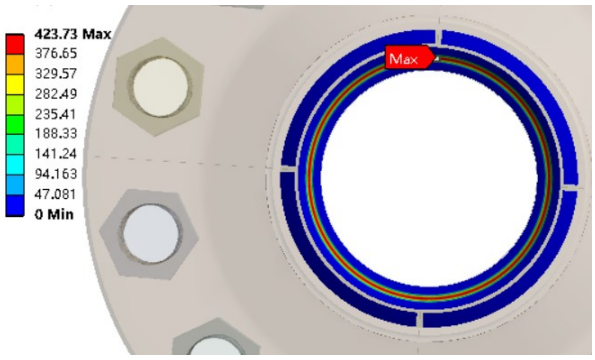

(c) Contact pressure cloud diagram of the non-optimized sealing structure at 125°C

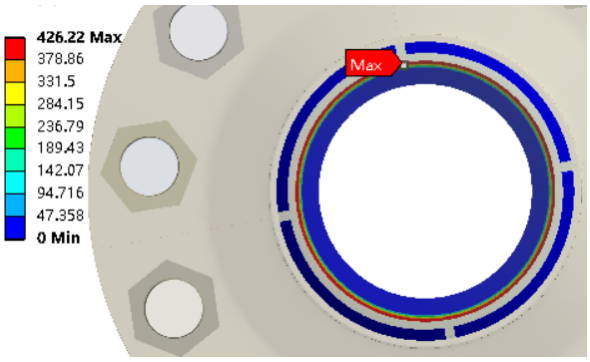

(d) Contact pressure cloud diagram of the optimized sealing structure at 125°C

Fig.8 Contact pressure cloud diagram of the sealing structure with two limit temperatures under the design pressure of 34.5 MPa

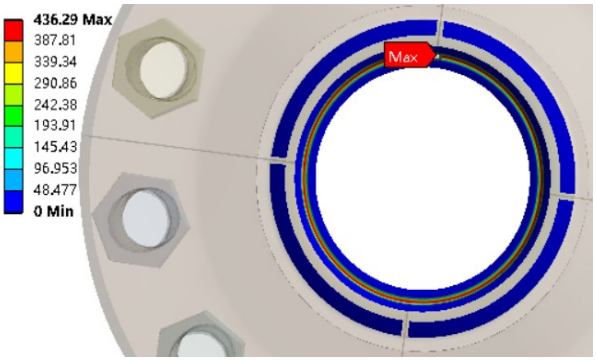

(a) Contact pressure cloud diagram of the non-optimized sealing structure at 25°C

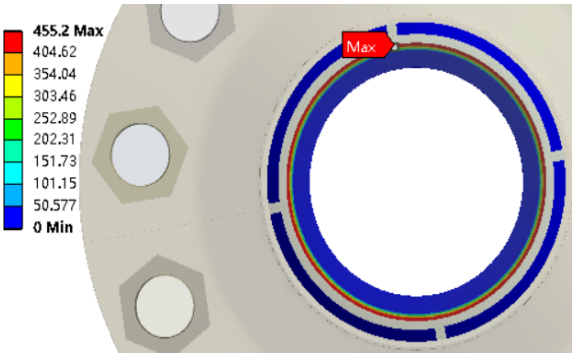

(b) Contact pressure cloud diagram of the optimized sealing structure at 25°C

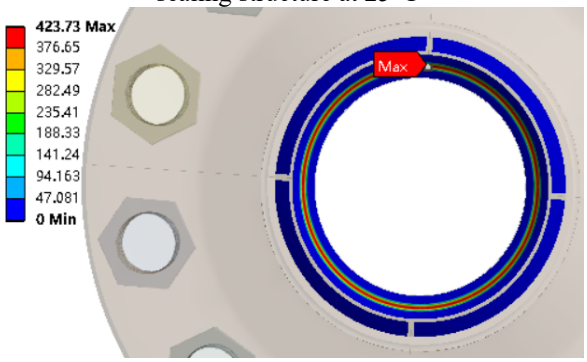

(c) Contact pressure cloud diagram of the non-optimized sealing structure at 125°C

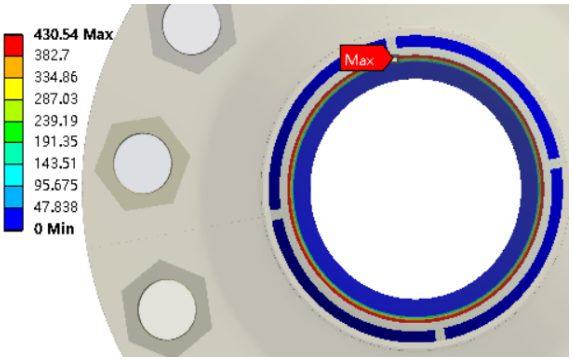

(d) Contact pressure cloud diagram of the optimized sealing structure at 125°C

Fig.9 Contact pressure cloud diagram of the sealing structure with two limit temperatures under the design pressure of 41.4 MPa

The cloud diagram of the contact pressure of non-optimized and optimized sealing structures at 25 °C and 125 °C under the design pressure of 41.4 MPa is given in Figure 9.

As can be seen from the two figures, the maximum contact pressure of the sealing structure under other combination conditions was more than twice the yield strength of the lenticular gasket material, which met the sealing judgment basis of the offshore flange connector, and the maximum contact pressure formed a 360° annular stress band, effectively preventing the radial leakage of crude oil.

Figures 10 and 11 depict the maximum contact pressure of the sealing structure under the condition of the two design pressures and various operating temperatures.

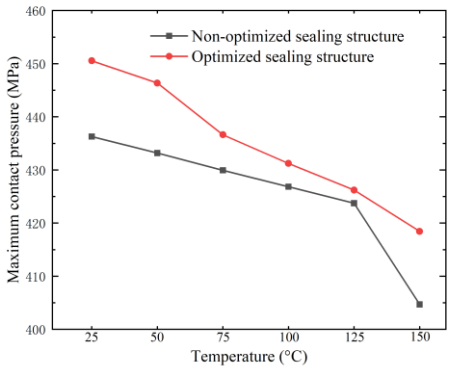

Fig.10 Contact pressure diagram of 34.5 MPa

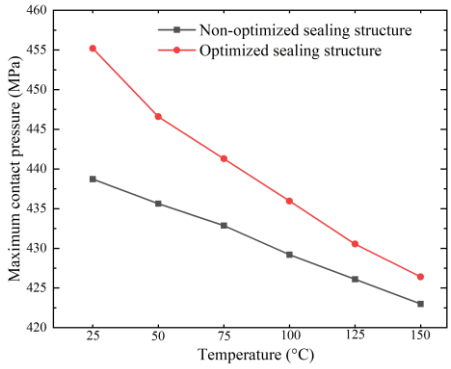

Fig.11 Contact pressure diagram of 41.4 MPa

Figures 10 and 11 show that: 1) The maximum contact pressure of non-optimized and optimized sealing structures decreased with the increase in operating temperature, because the higher the operating temperature, the lower the elastic modulus of the flange and the lenticular gasket materials, and the smaller the maximum contact pressure of the sealing surface [28]; 2) Under the design pressure of 34.5 MPa, the maximum contact pressure of non-optimized sealing structure did not meet the sealing judgment basis at the operating temperature of 150 °C, but it is not the same case with that under other working conditions; 3) The maximum contact pressure of optimized sealing structure exceeded that of non-optimized sealing structure at each operating temperature under the two design pressures, and thus satisfied the sealing judgment basis at each operating temperature. 4) As shown in Figure 10, under the design pressure of 34.5 MPa, the contact pressure of the optimized sealing structure increased by 3.4% at the maximum, 0.6% at the minimum, and 2.2% on average compared with that of the non-optimized sealing structure, It can be seen from Figure 11 that under the design pressure of 41.4 MPa, the contact pressure of the optimized sealing structure increased by 11.8% at the maximum, 2.3% at the minimum, and 5.9% on average compared with that of the non-optimized sealing structure.

As can be seen from Figures 12 and 13, the maximum equivalent pressure of the offshore flange connector emerged on the contact sealing surface between the flange and the lenticular gasket. The cloud map of the maximum equivalent pressure at two limit temperatures under two design pressures serves as an illustration.

As can be seen from Figures 12 and 13, the maximum equivalent pressure of the offshore flange connector emerged on the contact sealing surface between the flange and the lenticular gasket. The cloud map of the maximum equivalent pressure at two limit temperatures under two design pressures serves as an illustration.Under the two design pressures, the maximum equivalent pressure of the offshore flange connector at two limit temperatures was lower after optimization compared to that before optimization, and the optimized offshore flange connector was less likely to be damaged. Figurse 14 and 15 depict the maximum equivalent pressure distribution of offshore flange connector for each operating temperature under the two design pressures.

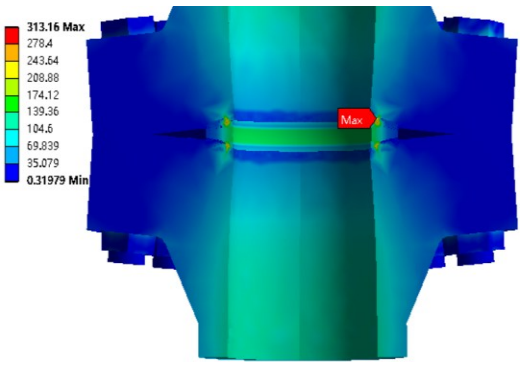

(a) Equivalent stress cloud diagram of the non-optimized sealing structure at 25°C

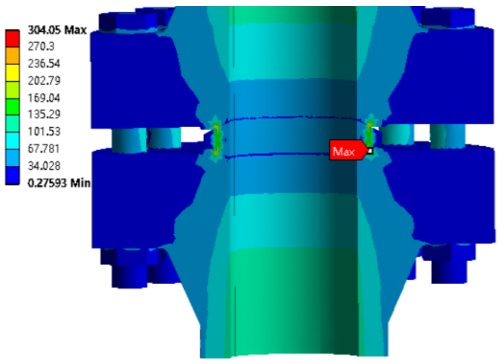

(b) Equivalent stress cloud diagram of the optimized sealing structure at 25°C

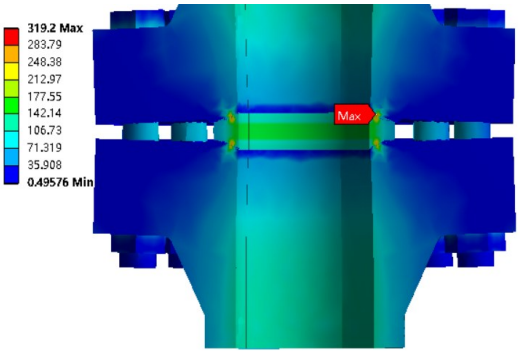

(c) Equivalent stress cloud diagram of the non-optimized sealing structure at 125°C

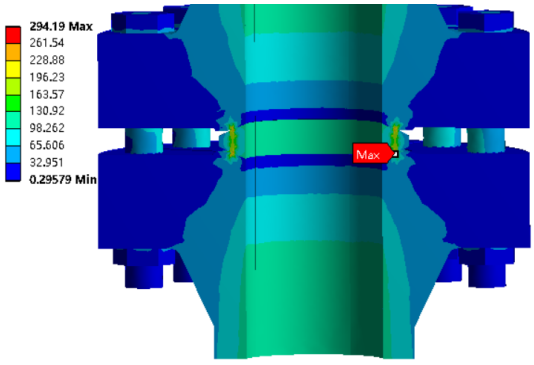

(d) Equivalent stress cloud diagram of the optimized sealing structure at 125°C

Fig.12 Equivalent stress diagram of the offshore flange connector under design pressure of 34.5 MPa

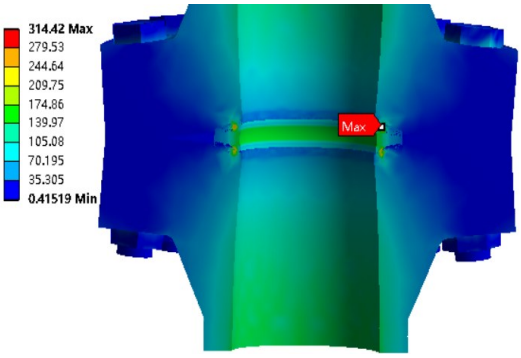

(a) Equivalent stress cloud diagram of the non-optimized sealing structure at 25°C

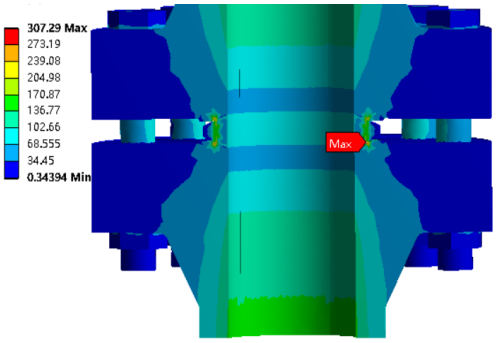

(b) Equivalent stress cloud diagram of the optimized sealing structure at 25°C

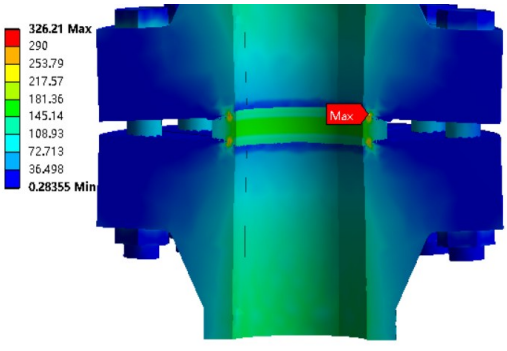

(c) Equivalent stress cloud diagram of the non-optimized sealing structure at 125°C

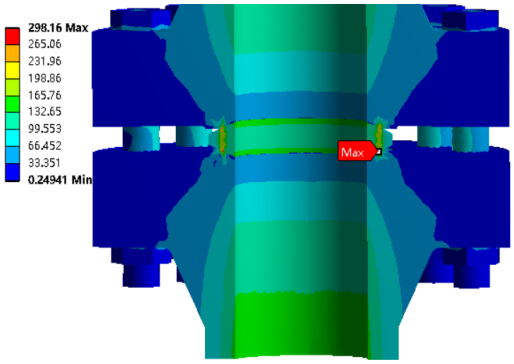

(d) Equivalent stress cloud diagram of the optimized sealing structure at 125°C

Fig.13 Equivalent stress diagram of offshore flange connector under design pressure of 41.4 MPa

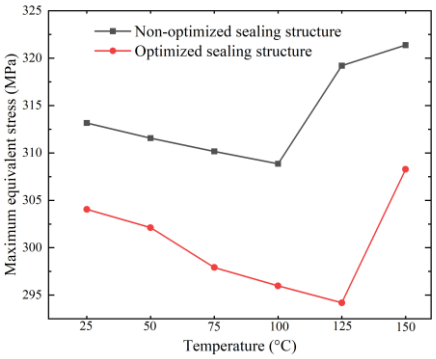

Fig.14 Maximum Equivalent Stress diagram of non-optimized and optimized sealing structure under design pressure of 34.5 MPa

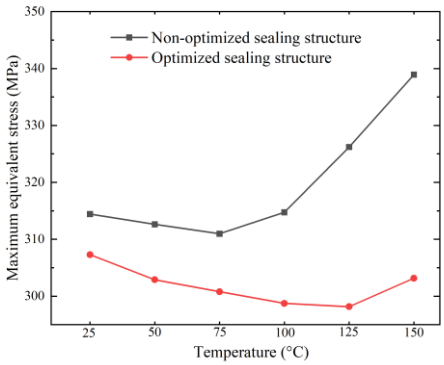

Fig.15 Maximum Equivalent Stress diagram of non-optimized and optimized sealing structure under design pressure of 41.4 MPa

As can be observed from the two figures, 1) The maximum equivalent pressure of the non-optimized and optimized offshore flange connectors under the two design pressures initially decreased and then increased with the increase in the operating temperature, because the materials of the flange and the lenticular gasket shows high brittleness at low temperatures, with a large binding force between molecules, and thus are easy to break. At this time, pressure concentration and crack propagation led to the maximum reduction in equivalent pressure in the pressure concentration area. When the offshore flange connector worked at high temperature, the activity of metal atoms between the sealing contact surface increased, the materials of flange and lenticular gasket started to change from brittleness to toughness, and as metal material is more prone to plastic deformation, and the maximum equivalent pressure in the contact stress concentration area began to rise with the increase of thermal stress; 2) At each operational temperature, the maximum equivalent pressure of the optimized offshore flange connector was lower than that of the non-optimized offshore flange connector. As shown in Figure 14, the maximum equivalent pressure of the optimized offshore flange connection decreased by 3% at the minimum, 8.5% at the maximum, and 4.6% on average compared with that of the non-optimized offshore flange connector at the design pressure condition of 34.5 MPa. As shown in Figure 15, the maximum equivalent pressure of the optimized offshore flange connection decreased by 2.3% at the minimum, 11.8% at the maximum, and 5.9% on average compared with that of the non-optimized offshore flange connector at the design pressure of 41.4 MPa. The smaller the maximum equivalent pressure, the less likely the offshore flange connector was to be damaged; 3) In terms of the non-optimized sealing structure, the inflection point of the maximum equivalent pressure changed with temperature at about 100 °C under the design pressure of 34.5 MPa and that at about 75 °C under the design pressure of 41.4 MPa; The optimized sealing structure inflected at approximately 125 °C under the two design pressures.

The horizontal ordinate interval of each numerical point in Figures 14 and 15 25° C. In order to further identify the precise inflection point, simulation was carried out at the interval of 1 °C close to each point. The numerical point at the interval of 1 °C was much more accurate than that at the interval of 25 °C, making it possible to determine the precise inflection point of the maximum equivalent pressure. The inflection points of the maximum equivalent pressure of the non-optimized and optimized sealing structures are respectively amplified in Figures 16 and 17.

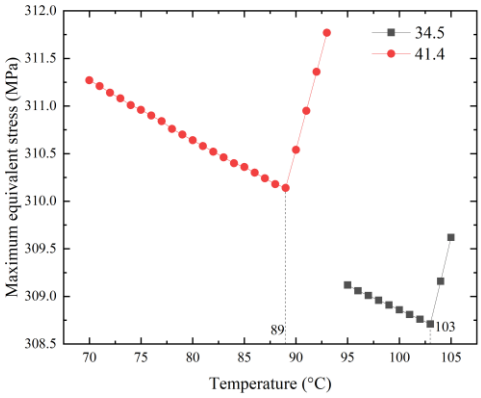

Fig.16 The inflection point of the maximum equivalent stress of the non-optimized sealing structure

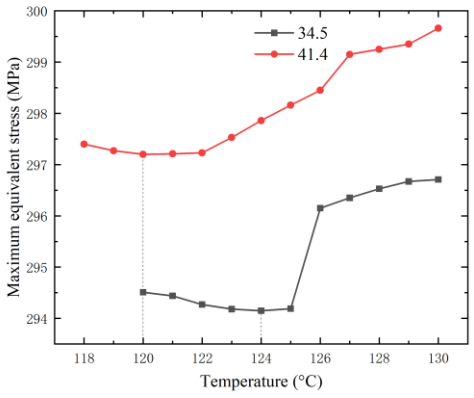

Fig.17 The inflection point of the maximum equivalent stress of the optimized sealing structure

As can be seen in Figure 15, the maximum equivalent pressure of the non-optimized sealing structure exhibited an inflection point at a temperature of 103 °C under the design pressure of 34.5 MPa, while that of the non-optimized sealing structure has an inflection point exhibited an inflection point at a temperature of 103 °C under the design pressure of 41.4 MPa. As can be seen from Figure 16, the maximum equivalent pressure of the optimized sealing structure exhibited an inflection point at a temperature of 125 °C under the design pressure of 34.5 MPa, while that of the non-optimized sealing structure has an inflection point exhibited an inflection point at a temperature of 120 °C under the design pressure of 41.4 MPa. Combined with the two figures, the inflection point for both the non-optimized and optimized sealing structures was delayed under the design pressure of 34.5 MPa compared to that under the design pressure of 41.4 MPa, indicating that the larger the pressure difference, the farther the inflection point, the larger the rising interval of the maximum equivalent pressure, and the more inclined the sealing structure towards failure. The maximum equivalent pressure of the optimized sealing structure was lower than that of the non-optimized sealing structure at the inflection points under the two design pressures. The increase range of the equivalent pressure by thermal stress is constrained by how far the inflection point delays. The maximum equivalent pressure of the optimized offshore flange connector was lower than that of the non-optimized offshore flange connector at high operating temperatures, which indicates that the optimized sealing structure was less susceptible to damage during high-temperature operation.

5. Conclusion

The optimal design model of the sealing structure of offshore flange connector was built in this study, and its optimal dimension was determined by the fmincon function in MATLAB software. Additionally, using Workbench software, the maximum equivalent pressure and maximum contact pressure of the non-optimized and optimized offshore flange connectors were compared and analyzed under the cross-combination of pressure and temperature factors, and the sealing performance of the non-optimized and optimized sealing structures was compared using the sealing judgment basis established in this paper. The following conclusions are drawn:

(1) The biggest innovation of this paper is to obtain the optimal dimension of the sealing structure through computer programming, which provides a theoretical reference for further improving the sealing structure of offshore flange connector. The optimized flange cone angle is 3.8° higher than that of the non-optimized one, and the curvature radius of the contact surface of the optimized lenticular gasket is 20 mm less than that of the non-optimized one. By maximizing the flange cone angle and the curvature radius of the contact surface of lenticular gasket, the sealing performance of the offshore flange connector is improved.

(2) The maximum contact pressure of the optimized sealing structure meets the sealing judgment basis of the offshore flange connector under the combination of two pressures and six temperatures. The maximum

contact pressure of the optimized sealing structure is greater than that of the non-optimized sealing structure, resulting in its better sealing performance.

(3) The maximum equivalent pressure of the optimized sealing structure is lower than the maximum equivalent stress of the non-optimized offshore flange connector. Moreover, compared with the non-optimized sealing structure, the inflection point of maximum equivalent pressure of the optimized sealing structure with temperature changes lags behind, with a smaller increase range caused by thermal stress and relatively low maximum equivalent pressure, making it difficult to destroy under actual working conditions. In the future, offshore flange connector should be developed to adapt to greater operating water depths, resist greater pressure shocks and be easier to install.

Acknowledgement

The authors sincerely acknowledge the support from the Natural Science Foundation of Inner Mongolia Autonomous Region (2023LHMS05029), and the Key R&D Program of Shandong Province (2021JMRH0322).

REFERENCES

[1] Zhou, X. K., Chen, J. H., Ge, Z.G., Zhao, T., Li, W. H.,2022. Numerical investigations on the effects of seabed shallow soils on a typical deepwater subsea wellhead system. *Brodogradnja*, 73(3), 1-19. https://doi.org/10.21278/brod73301

[2] Duan, M. L., Zhang, K., Soares, C. G., Paik, J. K., 2020. Theoretical investigation on hub structure design of subsea connectors. *Thin-Walled Structures*, 59(2), 107036. https://doi.org/10.1016/j.tws.2020.107036

[3] Wang, F. R., Zheng, C., Song G. B., 2021. A concept of underwater multi-bolt looseness identification using entropy-enhanced active sensing and ensemble learning. *Mechanical Systems and Signal Processing*, 149, 107186. https://doi.org/10.1016/j.ymssp.2020.107186

[4] Song, W. T., Cui, W. C., 2021. An overview of underwater connectors. *Journal of Marine Science and Engineering*, 9(8), 813. https://doi.org/10.3390/jmse9080813

[5] Robbe-valloire, F., Prat, M., 2008. A model for face-turned surface microgeometry application to the analysis of metallic static seals. *Wear,* 264(11–12), 980–989. https://doi.org/10.1016/j.wear.2007.08.001

[6] Yuan, Y., Xu, K., Zhao, K., 2020. The loading–unloading model of contact between fractal rough surfaces. *International Journal of Precision Engineering and Manufacturing*, 21(6), 1047-1063. https://doi.org/10.1007/s12541-020-00330-y

[7] Zhao, H. L., Chen, R., Luo, X. L., Duan, M. L., Lu, Y. H., Fu, G. W., Tian, H. P., Ye, D. H., 2015. Metal sealing performance of subsea X-tree wellhead connector sealer. *Chinese Journal Mechanical. Engineering*, 28, 649–656. https://doi.org/10.3901/CJME.2015.0309.026

[8] Jing, S., Mu, A., Zhou, Y., Xie, L., 2020. Finite-element analysis and structure optimization of X-O composite seal of cone bit. *Advances in Mechanical Engineering*. 12(5), 1-12. https://doi.org/10.1177/1687814020918686

[9] Li, Y. F., Zhao, H. L., Wang, D. G., Xu, Y. B., 2020. Metal sealing mechanism and experimental study of the subsea wellhead connector. *Journal of the Brazilian Society of Mechanical Sciences and Engineering.* 42, 26. https://doi.org/10.1007/s40430-019-2112-1

[10] Guo, Z. N., Li, H., Chang, G., 2022. Finite element analysis and structural optimization of V-shaped seal ring based on ANSYS Workbench. *Journal of Physics: Conference Series*, 2383, 012106. https://doi.org/10.1088/1742-6596/2383/1/012106

[11] Yang, M., Xia, Y. M., Ren, Y., Zhang, B. W., Wang, Y., 2023. Design of O-ring with skeleton seal of cutter changing robot storage tank gate for large diameter shield machine. *Tribology International*, 185, 108591. https://doi.org/10.1016/j.triboint.2023.108591

[12] Huang, Z. Q., Li, G., 2018. Optimization of cone bit bearing seal based on failure analysis. *Advances in Mechanical Engineering*, 10(3), 1-12. https://doi.org/10.1177/1687814018767485

[13] Cheng, T. F., Li, S. X., 2021.Structural Parameter Analysis of Self-Tightening Metal U-Shaped Seal Ring. *IOP Conference Series: Materials Science and Engineering*. 1081, 012001. https://doi.org/10.1088/1757-899X/1081/1/012001

[14] Ren, J., Zhu, H. W., Wang, H., Zhao, C. F., Zhong, J. L., 2020.Multi-objective Structural Optimization of VL Seal Ring Based on Isight. *Journal of Physics: Conference Series*, 1622, 012031. https://doi.org/10.1088/1742-6596/1622/1/012031

[15] Farkas, A., Degiuli, N., Martić, I., 2018. Assessment of hydrodynamic characteristics of a full-scale ship at different draughts. *Ocean Engineering*, 156, 135-152. https://doi.org/10.1016/j.oceaneng.2018.03.002

[16] Gong, H. X., Xu, Z. G., Shi, C. W., Wang, S., 2015.Analysis on self-tightening capacity of metal lens gasket connected by bolted flanges. *Journal of Huazhong University of Science and Technology (Natural Science Edition)*, 43(3), 123-127.

[17] Wang, L. Q., Wei, Z. L., Yao, S. M., Guan, Y., Li, S. K., 2018. Sealing Performance and Optimization of a Subsea Pipeline Mechanical Connector. *Chinese Journal of Mechanical Engineering*, 31, 18. https://doi.org/10.1186/s10033-018-0209-6

[18] Wang, L. Q., Wei, Z. L., Guan, Y., Li, S. K., 2016. A novel subsea pipeline connection method and experimental study. *Proceedings of the 26th International Ocean and Polar Engineering Conference*, Rhodes, Greece, 26 June-1 July, 907-913.

[19] Bucher., 1988. Industrial sealing technology. *Beijing: Chemical Industry Press*. (in Chinese).

[20] Gong, H. X., Xu, Z. G., Wang, S., 2015. A model for analysing the self-tightening coefficient of a metallic lenticular ring gasket joined by a bolted flange. *Material Research Innovations*, 19(suppl.6), S6-153. https://doi.org/10.1179/1432891715Z.0000000001469

[21] Zhang, D. Y., Xia, Y., Scarpa, F., Hong, J., Ma, Y. H., 2017. Interfacial contact stiffness of fractal rough surfaces. *Scientific Reports*, 7, 12874. https://doi.org/10.1038/s41598-017-13314-2

[22] Yun, F. H., Liu, D., Xu, X. J., Jiao, K. F., Hao, X. Q., Wang, L. Q., Yan, Z. P., Jia, P., Wang, X. Y., Liang, B., 2022. Thermal–structural coupling analysis of subsea connector sealing contact. *Applied Sciences*, 12(6), 3914. https://doi.org/10.3390/app12063194

[23] Wu, D., Wang, S. P., Wang, X. J., 2017. A novel stress distribution analytical model of O-ring seals under different properties of materials. *Journal of Mechanical Science and Technology*, 31, 289-296. https://doi.org/10.1007/s12206-016-1231-1

[24] Krishna, M. M., Shunmugam, M. S., Prasad, N. S., 2007.A study on the sealing performance of bolted flange joints with gaskets using finite element analysis. *International Journal of Pressure Vessels & Piping*, 84(6), 349-357. https://doi.org/10.1016/j.ijpvp.2007.02.001

[25] Zhang, Y., Li, D. Q., Hong, S. H., Zhang, M., 2023. Design of a new oscillating-buoy type wave energy converter and numerical study on its hydrodynamic performance. *Brodogradnja*, 74(1), 145-168. https://doi.org/10.21278/brod74108

[26] Liu, D., Yun, F. H., Wang, W. C., Jiao, K. F., Wang, L. Q., Yan, Z. P., Jia, P., Wang, X. Y., Liu, W. F., Sun, H. T., Xu, X. J., 2022. Sealing contact transient thermal-structural coupling analysis of the Subsea Connector. *Machines*, 10(3), 213. https://doi.org/10.3390/machines10030213

[27] Wang, W. C., Yun, F. H., Sun, H. T., Wang, L. Q., Yan, Z. P., Wang, G., Gong, H. X., Jiao, K. F., Liu, D., Hao, X. Q., 2021. The research and experiments on contact sealing theory of the underwater clamp connector. *Machines*, 9(11), 262. https://doi.org/10.3390/machines9110262

[28] Liu, L., Zhang, B. J., Zhang, H., Tang, H. L., Wang, W. J., 2023. Hydrodynamic performance optimization of marine propellers based on fluid-structure coupling. *Brodogradnja*, 74(3), 145-164. https://doi.org/10.21278/brod74308